Table I. Charge-Transfer Spectral Assignments for (Methylamine)cobalt(III) Complexes[a]

complex	$10^{-3}\nu_{max}$(calc), cm^{-1}	$10^{-3}\nu_{max}$(obs), cm^{-1} ($10^{-3}\epsilon$, M^{-1} cm^{-1})	assgnt
$Co(NMeH_2)_6^{3+}$	45.12	44.44 (31.0)	N → Co
$Co(NMeH_2)_5Cl^{2+}$	43.55	42.28[b] (26.6)	N → Co
	41.15		Cl(σ) → Co[c]
$Co(NMeH_2)_5Br^{2+}$	43.07	44.51 (18.1)	N → Co
	36.77	37.85 (18.0)	Br(σ) → Co[c]

[a] Measured in 10 °C acidic (pH ~ 3.2) solution. [b] Overlapping of N → Co and Cl → Co absorption bands occurs. [c] σ refers to an electron in an orbital having σ-symmetry with respect to the metal-ligand bond.

Table II. Quantum Yields and Product Ratios for Photoredox Reactions of (Methylamine)cobalt(III) Complexes

complex	λ_{excit}, nm	$\phi_{Co^{2+}}$[a] ($NMeH_2/Co^{2+}$)[b]	
		Ar purged	air-saturated
$Co(NMeH_2)_6^{3+}$	254	0.70 ± 0.03 (5.89 ± 0.13)	0.45 ± 0.03 (5.20 ± 0.07)
$Co(NMeH_2)_5Cl^{2+}$	254	0.54 ± 0.02 (4.91 ± 0.07)	0.40 ± 0.02 (4.30 ± 0.20)
	313	0.29 ± 0.01	0.29 ± 0.01
$Co(NMeH_2)_5Br^{2+}$	229	0.59 ± 0.03	0.49 ± 0.01
	254	0.43 ± 0.01 (5.02 ± 0.40)	0.38 ± 0.03 (5.02 ± 0.35)
	313	0.32 ± 0.02	0.31 ± 0.01

[a] Quantum yield of Co^{2+} production measured in acidic (pH ~ 3.2) aqueous solution at 10 °C. [b] Ratio of (mol $NMeH_2$) to (mol Co^{2+}) in photolyte. Co^{2+} analysis: Vydra, F.; Pribil, R. *Talanta* **1960**, *4*, 44. $NMeH_2$ analysis: DeBernardo, S.; Weigele, M.; Toome, V.; Manhart, K.; Leimgruber, W.; Böhlen, P.; Stein, S.; Udenfriend, S. *Arch. Biochem. Biophys.* **1974**, *163*, 390.

of free $NMeH_2$ observed in deoxygenated solution presumably arises from radical disproportionation processes that regenerate the amine.[2,8]

Special note should be taken of the wavelength-dependent effect of oxygen on the photochemical behavior of the haloamine complexes. In both cases, O_2 decreases $\phi_{Co^{2+}}$ at shorter excitation wavelengths but causes little or no change at longer wavelengths (Table II). This behavior reflects the contributions of two photoactive LMCT excited states that undergo imperfect communication with one another. Thus preferential population of the N → Co state at shorter wavelengths leads to the production of radicals that can be scavenged by O_2 (vide supra), whereas longer wavelength irradiation favors population of the lower energy Cl → Co or Br → Co CT state, which undergoes redox chemistry (e.g., eq 2) unaffected by O_2. Very different behavior has been reported for the corresponding $Co(NH_3)_5X^{2+}$ complexes in that internal conversion from the N → Co CT state to the lower-lying X → Co CT state occurs with nearly unit efficiency.[3] Evidently, replacement of NH_3 by $NMeH_2$ alters the kinetic parameters of the N → Co state such that chemical reaction increases in importance relative to other relaxation processes. At least two plausible explanations for this ligand effect deserve consideration: (1) the N → Co excited states in the methylamine complexes intrinsically are more dissociative, that is, they possess weaker Co–N bonds, and (2) the hydrophobic methyl groups situated on the periphery of the charged complex reduce interaction with the solvent; one consequence of this decreased solvation is a lowering of the reorganizational barrer that must be surmounted during dissociation of the solvent-caged primary radical pair. Experimental tests of these explanations are underway in our laboratory.

Finally, the photoredox behavior of $Co(NMeH_2)_5Br^{2+}$ in a 1:1 (v/v) glycerol–water mixture was investigated at several excitation wavelengths. In striking contrast to the results obtained for $Co(NH_3)_5Br^{2+}$ under similar conditions,[5] we find smaller $\phi_{Co^{2+}}$ values in this mixed solvent than in aqueous solution at *all* wavelengths in the interval 313–229 nm. Consequently, primary photooxidation of the solvent plays an unimportant role in the LMCT photochemistry of the methylamine complexes at very high excitation energy. This result again suggests that the methyl groups on the coordinated nitrogen atoms shield the complex from the solvent. More generally, we propose that LMCT excited states in alkylamine complexes of the type considered here approach "molecular" behavior[9] more closely than their ammine counterparts.

Acknowledgment. We thank the U.S. National Science Foundation (Grant DMR-8715635) and the IBM Corp. for financial support and Dr. Guillermo Ferraudi for performing flash photolysis studies.

Department of Chemistry
University of Georgia
Athens, Georgia 30602

Scott K. Weit
Charles Kutal*

Received November 9, 1989

(9) That is, the energetics and kinetics of LMCT excited states in alkylamine complexes are less susceptible to solvent perturbation: Endicott, J. F.; Ferraudi, G. J.; Barber, J. R. *J. Am. Chem. Soc.* **1975**, *97*, 219.

Synthesis and Structural Characterization of a Polyoxovanadate Coordination Complex with a Hexametalate Core: $[(n\text{-}C_4H_9)_4N]_2[V_6O_{13}\{O_2NC(CH_2O)_3\}_2]$

The coordination chemistry of polyoxometalates has received considerable attention by virtue of the structural analogy of these species to metal oxide surfaces.[1-3] Although polyoxomolybdate coordination chemistry has witnessed a remarkable development in the past decade,[4] the chemistry of analogous covalent polyoxovanadate derivatives remains unexplored. By exploitation of the solubility of polyvanadate tetra-*n*-butylammonium salts soluble in aprotic, polar solvents,[5-7] the polyoxoalkoxyvanadate–oxalate complex $[(n\text{-}C_4H_9)_4N]_2[V_8O_8(OCH_3)_{16}(C_2O_4)]$[8] was recently prepared, suggesting that simple organic subunits may be incorporated into polyoxovanadate frameworks. Our efforts have been directed toward the synthesis of simple coordination com-

(1) Day, V. W.; Klemperer, W. G. *Science (Washington, D.C.)* **1985**, *228*, 533.
(2) Pope, M. T. *Heteropoly and Isopoly Oxometalates*; Springer-Verlag: New York, 1983.
(3) McCarron, E. M.; Whitney, J. F.; Chase, D. B. *Inorg. Chem.* **1984**, *23*, 3275.
(4) For recent representative studies, see: (a) Chilou, V.; Gouzerh, P.; Jeannin, Y.; Robert, F. *J. Chem. Soc., Chem. Commun.* **1987**, 1469. (b) Ma, L.; Liu, S.; Zubieta, J. *Inorg. Chem.* **1989**, *28*, 175. (c) McCarron, E. M.; Sleight, A. W. *Polyhedron* **1986**, *5*, 129.
(5) Day, V. W.; Klemperer, W. G.; Maltbie, D. J. *J. Am. Chem. Soc.* **1987**, *109*, 2991.
(6) Day, V. W.; Klemperer, W. G.; Yaghi, O. M. *J. Am. Chem. Soc.* **1989**, *111*, 5959.
(7) Day, V. W.; Klemperer, W. G.; Yaghi, O. M. *J. Am. Chem. Soc.* **1989**, *111*, 4519.
(8) Chen, Q.; Liu, S.; Zubieta, J. *Inorg. Chem.*, submitted for publication.

0020-1669/90/1329-1456$02.50/0

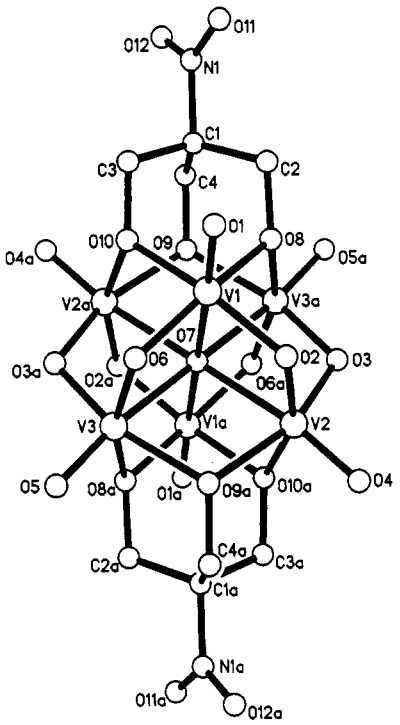

Figure 1. ORTEP view of the structure of $[V_6O_{13}\{O_2NC(CH_2O)_3\}_2]^{2-}$, showing the atom-labeling scheme. The central oxo group O7 sits at the crystallographic center of symmetry, such that the atoms labeled with the designator "a" are reflected to the unlettered atoms by symmetry. Selected bond lengths (Å) and angles (deg): V–O_t(av), 1.602 (4); V–O_b(av), 1.819 (4); V–O_c(av), 2.244 (2); V–O(alkoxy)(av), 2.028 (5); V–O_b–V(av), 109.7 (2); V–O(alkoxy)–V(av), 112.4 (2); V–O_c–V(av), 95.3 (2) and 84.7 (2). Abbreviations: O_t ≡ terminal oxo group; O_b ≡ doubly bridging oxo group; O_c ≡ central oxo group O7; O(alkoxy) ≡ bridging alkoxy donor of the $[O_2NC(CH_2O)_3]^{3-}$ ligand.

plexes of polyoxovanadates to provide a synthetic entry into this undeveloped class of compounds and to elucidate the structural consequences of ligand incorporation into the polyoxometalate framework, particularly with respect to degree of aggregation and to the identity of the polyoxo core. We report here the synthesis and structure of a polyhydroxylic derivative $[(n\text{-}C_4H_9)_4N]_2[V_6O_{13}\{O_2NC(CH_2O)_3\}_2]$, a complex possessing the hexametalate core, a structure previously observed in polyvanadate chemistry only for the organometallic species $[(C_5Me_5)Rh]_4(V_6O_{19})$.[9]

The reaction of $[(n\text{-}C_4H_9)_4N]_3[H_3V_{10}O_{28}]$ with tris(hydroxymethyl)nitromethane, $O_2NC(CH_2OH)_3$, in acetonitrile yields upon recrystallization lustrous red crystals of $[(n\text{-}C_4H_9)_4N]_2[V_6O_{13}\{O_2NC(CH_2O)_3\}_2]$ in 40% yield.[10] The stoichiometry of the reaction under optimal conditions conforms to the following equation:

$$2(TBA)_3H_3V_{10}O_{28} + 6O_2NC(CH_2OH)_3 \rightarrow 3(TBA)_2[V_6O_{13}\{O_2NC(CH_2O)_3\}_2] + 12H_2O + V_2O_5$$

The identity of the insoluble white powder V_2O_5, produced as a side product of the reaction, was confirmed by infrared spectroscopy. The reaction has proved general for the synthesis of complexes of the type $[V_6O_{13}\{RC(CH_2O)_3\}_2]^{2-}$, R = $-CH_3$, $-NO_2$, and –OH.[11] The hydroxy derivative provides a useful precursor for condensation reactions coupling hexavanadate cores and for silylation processes, allowing isolation of a variety of derivatives of the general class $[V_6O_{13}\{R_3SiOC(CH_2O)_3\}_2]^{2-}$.

X-ray structural analysis of crystalline $[(n\text{-}C_4H_9)_4N]_2[V_6O_{13}\{O_2NC(CH_2O)_3\}_2]$ (**1**)[12] revealed the presence of discrete $[(n\text{-}C_4H_9)_4N]^+$ cations and of molecular anions in which two $[O_2NC(CH_2O)_3]^{3-}$ subunits are bound to a $[V_6O_{13}]^{4+}$ core, as illustrated in Figure 1. Alternatively, the structure may be viewed as a hexametalate core $[V_6O_{19}]^{8-}$ supporting two $[O_2NC(CH_2)_3]^{3+}$ subunits. The ligand moieties occupy opposite faces of the $[V_6]$ octahedron.

Although the structural core is grossly similar to that reported for $[(C_5Me_5)Rh]_4(V_6O_{19})$, the metrical parameters observed for **1** reveal significant distortions from the more or less regular $[V_6O_{19}]^{8-}$ "superoctahedral" core of the Rh analogue. Thus, whereas the V–O_b distances of $[(C_5Me_5)Rh]_4[V_6O_{19}]$ are nearly equivalent (1.916 (4) Å, average) as are the V–O_b–V angles (111.9 (3)°, average), the V–O bridging distances in **1** are significantly different for doubly bridging oxo groups and bridging alkoxy units, 1.819 (4) and 2.028 (5) Å, respectively, a feature paralleled by the V–O–V angles of 109.7 (2) and 112.4 (2)° for bridging oxo and alkoxy donors, respectively.

Hexametalate species generally exhibit well-behaved electrochemical properties, and **1** is no exception. Cyclic voltammetric studies of solutions 0.1 M in $(n\text{-}C_4H_9)_4NPF_6$ and 0.001 M in **1** reveal a reversible one-electron reduction at –0.60 V relative to the ferrocene/ferrocenium couple.[13] Controlled-potential electrolysis at –0.85 V confirms the one-electron reduction, which is accompanied by a change from the light red solution of $[V_6O_{13}\{O_2NC(CH_2O)_3\}_2]^{2-}$ to dark brown of $[V_6O_{13}\{O_2NC(CH_2O)_3\}_2]^{3-}$.[14] The EPR spectrum of the reduced anion at 77 K exhibits a broadened eight-line pattern with $A(^{51}V)$ = 103 G, centered at g = 2.049.

The characterization of **1** suggests that the coordination chemistry of polyoxovanadates in accessible but may not directly parallel that observed for polyoxomolybdates. Furthermore, the observation of the $[V_6O_{19}]^{8-}$ core for both organometallic and coordination complexes demonstrates that the core may be prevalent in the chemistry of oxovanadates and that significant variation in the structural parameters associated with the core may be tolerated.

Acknowledgment. This work was supported by NSF Grant CHE8815299.

(9) (a) Chae, H. K.; Klemperer, W. G.; Day, V. W. *Inorg. Chem.* **1989**, *28*, 1423. (b) Hayashi, Y.; Ozawa, Y.; Isobe, K. *Chem. Lett.* **1989**, 425.

(10) All manipulations were carried out in an N_2 atmosphere. Tris(hydroxymethyl)nitromethane (0.454 g, 0.003 mol) was added to a solution of $[(n\text{-}C_4H_9)_4N]_3[H_3V_{10}O_{28}]$ (3.38 g, 0.002 mol) in CH_3CN (50 mL) with stirring. The yellow-brown solution obtained upon refluxing for 24 h was cooled to room temperature and reduced in volume to 30 mL by rotary evaporation. Upon addition of 30 mL of diethyl ether, a reddish brown powder was obtained (1.45 g). Recrystallization from DMF/CH_3CN/diethyl ether (1:1:2 v/v/v) yielded red crystals in 40–45% yield. The crystalline product is indefinitely stable when exposed to the atmosphere, while solutions of the complex decompose over a period of days when exposed to the atmosphere at room temperature. Anal. Calcd for $C_{40}H_{84}N_4O_{23}V_6$: C, 37.1; H, 6.49; N, 4.33. Found: C, 37.2; H, 6.32; N, 4.26. IR (KBr pellet, cm^{-1}): 2959 (m), 1531 (m), 1335 (w), 1260 (s), 1083 (s), 1022 (m), 960 (m), 944 (s), 800 (s), 719 (m), 410 (m).

(11) Satisfactory elemental analyses and X-ray crystal structures have been obtained for the $-CH_3$ and –OH derivative also. Crystal data for $(TBA)_2[V_6O_{13}\{CH_3C(CH_2O)_3\}_2]$: triclinic space group $P\bar{1}$, a = 11.460 (2) Å, b = 12.237 (2) Å, c = 12.331 (3) Å, α = 62.89 (1)°, β = 63.50 (1)°, γ = 77.52 (1)°, V = 1377.4 (8) Å^3, Z = 2. Structure solution and refinement based on 2428 reflections with $F_o \geq 6\sigma(F_o)$ (Mo Kα radiation, λ = 0.71073 Å) converged at an R value of 0.0561. Crystal data for $(TBA)_2[V_6O_{13}\{HOC(CH_2O)_3\}_2]$: monoclinic space group $P2_1/c$, a = 12.003 (3) Å, b = 16.900 (3) Å, c = 16.769 (3) Å, β = 106.95 (1)°, V = 3253.8 (10) Å; 3848 reflections, R = 0.0544 (conditions as above). The complexes are isostructural with the $-NO_2$ derivative.

(12) Crystal data at 233 K: triclinic space group $P\bar{1}$, a = 11.470 (2) Å, b = 12.149 (3) Å, c = 12.433 (2) Å, α = 63.24 (1)°, β = 63.45 (1)°, γ = 79.31 (2)°, V = 1383.7 (5) Å^3, Z = 1 (hexamer), D_{calc} = 1.55 g cm^{-3}. A total of 5756 reflections with $2\theta < 50°$ (Mo Kα radiation, λ = 0.71073 Å) were collected on a Nicolet R3mV diffractometer using $\theta/2\theta$ scans. Of these, 4447 reflections with $F_o \geq 6\sigma(F_o)$ were used in the structure solution and refinement, resulting in a final discrepancy factor of 0.0515.

(13) The cyclic voltammetric measurements were carried out on a BAS electrochemical analyzer. The cell had platinum working and auxiliary electrodes; a silver wire served as a pseudo-reference electrode, with ferrocene/ferrocenium (fe/fe$^+$) serving as the internal calibrant. For complex **1**, $E_{1/2}$ = –0.60 V with ΔE = 70 mV and i_{pc}/i_{pa} = 1.00. For the fe/fe$^+$ couple, ΔE = 70 mV and i_{pc}/i_{pa} = 1.00.

(14) Electronic spectra, CH_3CN solvent [λ_{max}, nm (ϵ, M^{-1} cm^{-1})]: $[(n\text{-}C_4H_9)_4N]_2[V_6O_{13}\{O_2NC(CH_2O)_3\}_2]$, 226 (3.6 × 10^4), 248 (2.9 × 10^4), 312 (1.7 × 10^4); $[(n\text{-}C_4H_9)_4N]_3[V_6O_{13}\{O_2NC(CH_2O)_3\}_2]$, 231 (1.1 × 10^4), 252 (9.8 × 10^3), 305 (6.2 × 10^3), 402 (1.9 × 10^3), 504 (6.4 × 10^3).

Supplementary Material Available: Tables S1-S5 and S78, listing fractional atomic coordinates for non-hydrogen atoms, bond lengths, bond angles, anisotropic temperature factors for all non-hydrogen atoms, calculated atomic positions for hydrogen atoms, and crystallographic experimental conditions (9 pages); Table S6, listing observed and calculated structure factors (18 pages). Ordering information is given on any current masthead page.

Department of Chemistry
State University of New York at Albany
Albany, New York 12222

Qin Chen
Jon Zubieta*

Received November 21, 1989

Crystal Structure of $LiNb(OCH_2CH_3)_6$: A Precursor for Lithium Niobate Ceramics

Metal alkoxide complexes have received renewed attention as precursors for metal oxides.[1] A recent application toward ceramic materials, "sol-gel" processing, uses the tendency of metal alkoxides to form polymeric structures upon hydrolysis.[2] Heat treatment of the resultant polymeric structures typically yields amorphous oxides that can be crystallized at higher temperatures.[3] An important example of sol-gel processing is the fabrication of lithium niobate, $LiNbO_3$, ceramics for applications such as optical modulation.[4] However, homogeneous material is a prerequisite in these applications, to eliminate variations in refractive index and electrical properties. Therefore, sol-gel processing has been investigated as a means of producing high-purity homogeneous material of the desired stoichiometric composition. The crystal structure of heterometallic alkoxides may be of particular interest to materials chemists investigating the evolution of molecular structure during sol-gel processing of metal oxides.

In this paper we report the crystal structure of lithium niobium ethoxide, $LiNb(OCH_2CH_3)_6$, which as been used in the preparation of lithium niobate.[5] Mehrotra has previously reported that the reaction of niobium and lithium alkoxides resulted in isolation of white powders corresponding to $LiNb(OR)_6$.[6] We have recently presented further *spectroscopic* evidence for the formation, in solution, of the heterometallic alkoxide lithium niobium ethoxide.[7] However, prior to this report, the *solid-state* structure of lithium niobium ethoxide had not been elucidated.

Equimolar quantities of lithium ethoxide[8] and niobium ethoxide[9] were reacted under reflux in a dry dinitrogen atmosphere for 24 h to give a solution of approximately 0.25 M concentration. Crystals were obtained at room temperature when the ethanolic solution was concentrated to approximately 1 M. The crystals thus obtained were transparent and 2-5 mm in length and were the subject of our crystallographic study.[10]

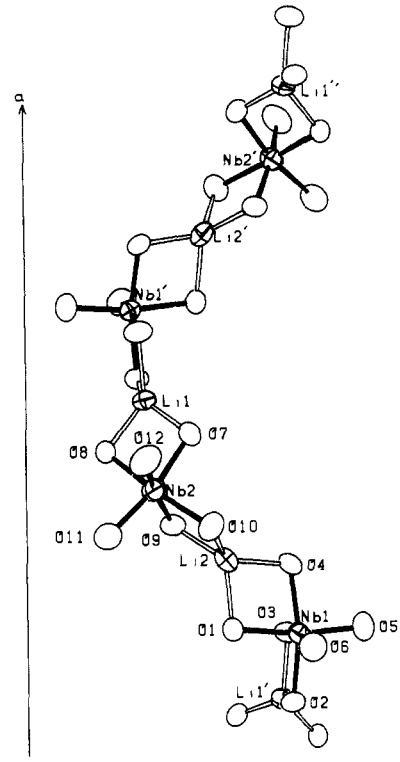

Figure 1. Thermal ellipsoid (35% probability) perspective view normal to the *a* axis, showing one translational unit (ORTEP-II). Carbon atoms were omitted for clarity.

The crystallographic asymmetric unit contains two independent Li atoms and two independent Nb complexes forming infinite helical $LiNb(OCH_2CH_3)_6$ polymers composed of alternating $Nb(OCH_2CH_3)_6$ octahedra cis-linked by (severely distorted) tetrahedral Li atoms. One cis pair of ethoxide ligands is terminal, while the remaining ligands form bis(μ-O) bridges with two Li atoms to generate the polymer (Figure 1). The centrosymmetric unit cell consists of alternating right- and left-handed helical polymers parallel to the *a* axis. There are no intermolecular

(1) See, for example: Bradley, D. C. *Chem. Rev.* **1989**, *89*, 1317. Johnson, D. W., Jr. *Am. Ceram. Soc. Bull.* **1985**, *64*, 1597. Roy, R. *Science* **1987**, *238*, 1664.
(2) See, for example: Bradley, D. C.; Mehrotra, R. C.; Gaur, D. P. *Metal Alkoxides*; Academic Press: London, 1978. Bradley, D. C. *Coord. Chem. Rev.* **1967**, *2*, 299. Dislich, H. *J. Non-Cryst. Solids* **1983**, *57*, 371.
(3) See, for example: Schwartz, R. W. Ph.D. Thesis, University of Illinois at Urbana-Champaign, 1989. Klein, L. C. *Sol-Gel Technology for Thin Films, Fibers, Preforms, Electronic and Specialty Shapes*; Noyes Publications: Park Ridge, NJ, 1988.
(4) Weis, R. S.; Gaylord, T. K. *Appl. Phys. A* **1985**, *37*, 191.
(5) Eichorst, D. J.; Payne, D. A. In *Better Ceramics Through Chemistry III*; Brinker, C. J., Clark, D. E., Ulrich, D. R., Eds.; Materials Research Society Symposium Proceedings 121; Materials Research Society: New York, 1988; p 773. Hirano, S. In *Ceramic Powder Science*; Proceedings of the International Conference on Ceramic Powder Processing Science; Messing, G. L., Fuller, E. R., Jr., Hausner, H., Eds.; American Ceramic Society: Westerville, OH, 1988; p 171. Partlow, D. P.; Greggi, J. *J. Mater. Res.* **1987**, *2*, 595. Puyôo-Castaings, N.; Duboudin, F.; Ravez, J. *J. Mater. Res.* **1988**, *3*, 557. Yanovskaya, M. I.; et al. *J. Mater. Sci.* **1988**, *23*, 395. Hirano, S. I.; Kato, K. *Adv. Ceram. Mater.* **1988**, *3*, 503.
(6) Mehrotra, R. C.; Agrawal, M. M.; Kapoor, P. N. *J. Chem. Soc. A* **1968**, 2673.
(7) Eichorst, D. J.; Howard, K. E.; Payne, D. A. In *Proceedings of Fourth International Conference on Ultrastructure Processing of Ceramics, Glasses and Composites*; Uhlmann, D. R., Weinberg, M. C., Risbud, S. H., Ulrich, D. R., Eds.; J. Wiley: New York, in press.
(8) Lithium metal (0.347 g, 0.050 mol) was added under N_2 to dry ethanol (100 mL, dried and distilled from magnesium) and stirred until all of the metal had been consumed.
(9) $Nb(OCH_2CH_3)_5$ was prepared according to: Bradley, D. C.; Chakravarti, B. N.; Wardlaw, W. *J. Chem. Soc.* **1956**, 2381. It was purified by successive crystallizations and vacuum distillation. A total of 15.91 g of $Nb(OCH_2CH_3)_5$ was added to 100 mL of dried absolute ethanol.
(10) Crystal data for $LiNb(OCH_2CH_3)_6$: transparent, colorless, equidimensional crystal, 0.3 × 0.3 × 0.4 mm, orthorhombic, space group *Pbca*, a = 17.704 (4) Å, b = 19.736 (5) Å, c = 21.267 (8) Å, V = 7431 (6) Å^3, ρ_{calc} = 1.324 g/cm^3, Z = 16, 198 K. Diffraction data: Enraf-Nonius CAD4 automated κ-axis diffractometer, monochromated Mo radiation ($\lambda(K\bar{\alpha})$ = 0.710 73 Å), range $2 < 2\theta < 46°$ ($+h,+k,+l$) and $2 < 2\theta < 8$ ($\pm h,\pm k,\pm l$), 6054 reflections (5154 unique, R_i = 0.020, 2200 observed, $I > 2.58\sigma(I)$); corrected for anomalous dispersion, Lorentz, and polarization effects but not for absorption (μ = 6.35 cm^{-1}). Solution: Patterson methods (SHELXS-86) located Nb atoms, difference Fourier syntheses gave positions for remaining non-hydrogen atoms (severely disordered alkyl groups). Refinement: (SHELX-76) H atom contributions ignored, normalized site occupancy factors for each ethyl group, common variables for C-O (1.47 Å) and C-C (1.50 Å) bond lengths, a common isotropic thermal parameter for carbon atoms, anisotropic thermal coefficients for non-carbon atoms. Final results: difference Fourier map (range $0.50 > e/Å^+ > -0.54$) located maximum residual electron density in vicinity of ethyl carbon atoms; variance between observed and calculated structure factors depended (slightly) on $\sin\theta$; agreement factors, R = 0.062 and R_w = 0.074.

0020-1669/90/1329-1458$02.50/0